Edelweiss Applied Science and Technology
ISSN: 2576-8484
Vol. 8, No. 6, 9555-9567
2024
Publisher: Learning Gate
DOI: 10.55214/25768484.v8i6.4035

Cluster analysis of rainfall patterns in Mamminasata: Validation of climate hazards group infrared precipitation with station dataset using observational comparisons

Nurtiti Sunusi[1*], Giarno[2], Muflihah[3], Sumanta Pasari[4]
[1]Stochastic Modeling Research Group Department of Statistics, Faculty of Mathematics and Natural Sciences, Hasanuddin University, Indonesia, 90245; nurtitisunusi@unhas.ac.id (N.S.).
[2]State College of Meteorology Climatology and Geophysics, Tangerang 15221, Indonesia.
[3]Meteorology, Climatology and Geophysical Agency of Indonesia, Makassar, Indonesia.
[4]Birla Institute of Technology and Science, Pilani, India.

Abstract: This study aims to apply the cluster method to objectively classify rainfall patterns in the Mamminasata monsoon region based on observational data and Climate Hazards Group InfraRed Precipitation with Station (CHIRPS) data. Validation was carried out using dichotomous and numerical comparisons with in situ observational data to strengthen the validity of CHIRPS data. The results showed that observational and CHIRPS data showed three different rainfall patterns. The first pattern shows rainfall at the beginning or end of the year ranging from 80-110 mm, decreasing after the 9th day of March, then increasing again in May to mid-June. The second pattern has a slightly lower rainfall intensity than the first one. The third pattern shows rainfall that increases beyond 100 mm at the end of each year, decreasing after February and reaching its lowest point in August. Towards the end of the year, there is an increase exponentially. CHIRPS rainfall predictions tend to overestimate in the southwest coastal area of Mamminasata, while underestimations are observed in the northern urban areas and eastern mountains. The accuracy of satellite rainfall estimates varies significantly across the Mamminasata region. In general, the performance of CHIRPS rainfall estimates is better in lowland areas than in mountainous areas.

Keywords: *CHIRPS, Mamminasata, Monsoonal, Rainfall pattern.*

1. Introduction

Indonesia, situated within the maritime continent, experiences a diverse rainfall pattern. The global circulation influences rainfall patterns in Indonesia. The occurrence of rainfall on the Indonesian marine continent (IMC) is significantly affected by global phenomena such as El Niño Southern Oscillation (ENSO), Madden Julian Oscillation (MJO), and Indian Ocean Dipole (IOD) [1]–[6]. As a result, rainfall in Indonesia varies from region to region. The rainy season makes Indonesia prone to flooding, while the dry season is prone to drought. Based on its rainfall type, Indonesia reveals three patterns, namely the monsoonal rainfall pattern, which has a peak rainfall in December, January, and February; the local pattern, with its peak rainfall in June, July, and August; and the equatorial pattern which experiences two peak rainfalls.

Mamminasata, which stands for the regions of Makassar, Maros, Sungguminasa, and Takalar, is a significant area in Indonesia. Makassar, the capital of South Sulawesi Province, is a bustling metropolis supporting the development of its surrounding regions, including Maros Regency, Gowa Regency, and Takalar Regency. This has led to a rapid population growth, reaching 2.88 million people in 2020. As a central hub for various activities, Mamminasata requires extensive urban infrastructure and facilities. With 8.7 million annual flights [7], it is an essential gateway to eastern Indonesia and attracts people for economic, educational, and cultural purposes. The urban area of Mamminasata was officially established in 2003, covering an area of 246,230 hectares. It was designated as a National Strategic Area

* Correspondence: nurtitisunusi@unhas.ac.id

through Government Regulation Number 26 of 2008 on the National Area Spatial Plan. Numerous strategies have been implemented to support the region's development. However, the swift growth has led to inadequate control over land use, impacting the area's resilience to natural changes [8]. Flooding has become a notable consequence of the region's dynamic weather conditions in recent times [9], [10].

Although the rainfall pattern in Mammimasata is monsoon, the flooding distribution in this city varies. Over the past five years, the Mamminasata Region has encountered multiple floods during the peak of the rainy season. The most devastating flood occurred on January 21, 2019, resulting in the loss of more than 50 people and being regarded as the most significant flood incident [11]. In this incident, the highest flood was located on the Maros-Makassar border. In early 2024, severe flooding occurred in the Makassar City area, but the Maros-Makassar border was unaffected. The severity of this flood has instilled concerns among people about its recurrence in the future. Reports on this incident highlighted that the Maros-Makassar border area suffered the worst impact. Therefore, it can be inferred that the flood-affected locations were not evenly distributed. Understanding the intensity of rainfall distribution patterns that can potentially contribute to flooding in this region is crucial since not all heavy rain events lead to floods or landslides [12].

The accuracy of weather observations is heavily influenced by the number and network of weather stations [13], [14]. Determining the observation network involves considering the shape and quantity of observation sites. Deciding on the required stations balances desired accuracy and cost considerations. The scarcity of rainfall measurements on the Earth's surface is primarily due to limitations such as limited funds, human resources, and challenging field conditions. Achieving a detailed analysis of rainfall at sub-district or village levels requires using dense rain gauges, which are currently unavailable in Indonesia. Developing remote-sensing rain observation technology can be a potential solution to address this issue. Using remote-sensing techniques makes it possible to gather rainfall data without solely relying on surface-based rain gauges. This technology offers an alternative approach to overcome the lack of distribution of rain gauges on the surface [15]–[18].

In remote sensing observations, rainfall is calculated using the knowledge of electromagnetic waves emitted by clouds and captured by satellites/radar. Satellite rainfall estimation can cover an extensive area with various spatial and temporal resolutions [19]. The advantages of satellites compared to surface observations are high spatial and temporal resolution and real-time [20], making it more economical. Some rainfall estimation results, such as Tropical Rainfall Measuring Mission [21], [22], Precipitation Estimation from Remotely Sensed Information using Artificial Neural Networks [23]–[25], and The Climate Prediction Center MORPHing technique [26], however, rainfall estimation results from these remote-sensing data vary in accuracy over space (place) and time [27]. Validation of CHIRPS rainfall estimates shows that CHIRPS performs well in estimating monthly and annual rainfall [28], [29].

Rainfall pattern recognition can be carried out using cluster techniques. This method has been widely used in various fields, including the classification of weather parameters [30]-[35]. Cluster analysis uses many variables grouped into similar objects to obtain groups with similar characteristics. Mamminasata, a densely populated area, requires more details about rainfall patterns that can be used in reasonable flood anticipation; however, the number of rain gauges is limited [13]. Rainfall estimates, such as CHIRPS, can be used as a substitute for in-situ data. However, its accuracy still needs to be tested, especially its daily performance. This study aims to apply the cluster method to objectively classify rainfall patterns in the monsoonal region of Mamminasata based on observation data and the CHIRPS data.

2. Materials and Methods

2.1. Study Area

The study area in this research is the Mamminasata Region, as shown in Figure 1. There are 48 observation stations used for test points. Most measurements were made in areas near the coast where the elevation is less than 50 meters above sea level. This study uses daily rainfall accumulation data from January 1, 1983 to December 31, 2023.

Edelweiss Applied Science and Technology
ISSN: 2576-8484
Vol. 8, No. 6: 9555-9567, 2024
DOI: 10.55214/25768484.v8i6.4035

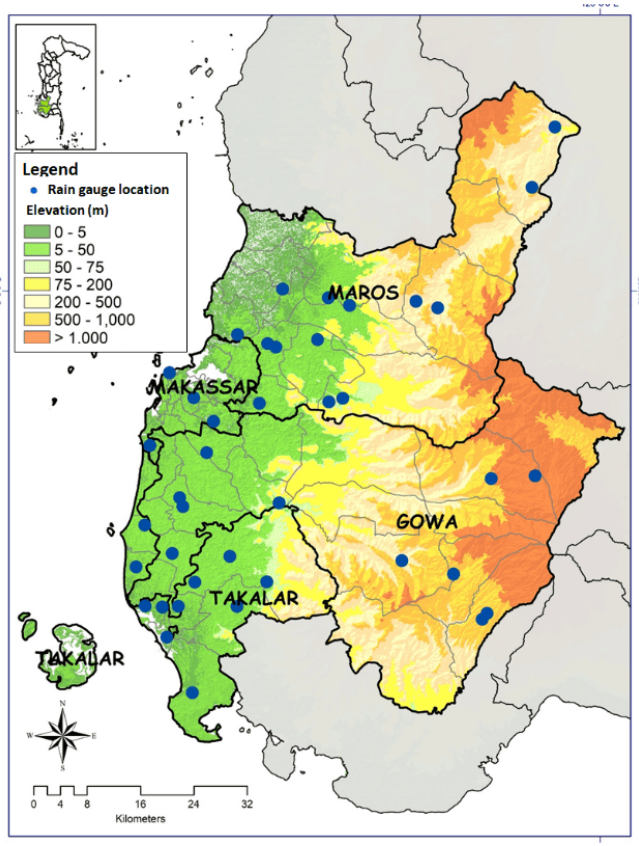

Figure 1.
Spreading rain gauge in the research location.

Not all monitoring locations initiate observations simultaneously due to staggered equipment installation. There are missing or vacant data since the data will be cross-referenced with the estimated CHIRPS rainfall data, which commences from January 1, 1983. These data gaps, however, arise not solely from the absence of observations but also stem from equipment malfunctions or other technical discrepancies. The recorded data and the disparity in observation periods have been rectified to address inaccuracies or errors. Data containing inaccuracies are treated on par with void or omitted data, and no comparison is drawn against the CHIRPS dataset.

2.2. Clustering Rainfall Pattern

Rainfall patterns in Indonesia are distinguished based on the subjective monthly rainfall graph [36]. By developing statistical methods, differences in several data can be classified using cluster analysis. Cluster analysis uses many variables grouped into similar objects to obtain groups with similar characteristics. This study calculates rainfall as its distance or (dis)similarity between each pair of variables. Suppose there are two elements (x, y), and then use the Euclidean distance in this research. Euclidean Distance measures the straight-line distance between two points in Euclidean space. It is calculated using the formula:

$$d_{euc}(x,y) = \sqrt{\sum_{i=1}^{n}(x_i - y_i)^2} \quad (1)$$

Where:

- x and y are two points in n-dimensional space, with coordinates $(x_1, x_2, \ldots, x_n)$ and $(y_1, y_2, \ldots, y)$.
- $d(x,y)$ is the Euclidean distance between p and q.

Edelweiss Applied Science and Technology
ISSN: 2576-8484
Vol. 8, No. 6: 9555-9567, 2024
DOI: 10.55214/25768484.v8i6.4035

2.3. Clustering Rainfall Pattern

The dichotomous method is used to evaluate the ability of CHIRPS to estimate rainfall events. This method describes two categories (dichotomous) of events in rainfall predictions and observations, namely the frequency of "Yes" or "No" events. Predictions or estimates are considered "Yes" if rainfall values exceed 0.5 mm/day. Conversely, if it is less than 0.5 mm/day, it is calculated as "No." The result is that the relationship between rainfall predictions and observations has four conditions: hits, false alarms, misses, and correct negatives [30]. Dichotomous has two-dimensional tables that describe the discrete distribution of a composite sample of a deterministic rainfall forecast estimate by CHIRPS and in-situ observations. The correspondence of hits, false alarms, misses, and correct negatives to CHIRPS predictions and rain observations is shown in Table 1.

Table 1.
Contingency Table Scheme used in the study.

		Rainfall observation		
		Yes	**No**	**Total**
CHIRPS	Yes	*hit* (a)	*false alarm* (b)	a+b
	No	*miss* (c)	*correct negative* (d)	c+d
	Sum	a+c	b+d	a+b+c+d=n

Evaluation of rainfall estimation capability is quantified using the calculation of Proportion Correct (PC), Hit Rate or Probability of Detection (POD), False Alarm Ratio (FAR), Frequency Bias (B), and Threat Score (TS) or Critical Success Index (SCI) values using the following equations:

$$PC = \frac{Hits+Correct\ Negatives}{Total} \quad (2)$$

$$POD = \frac{Hits}{Hits+Misses} \quad (3)$$

$$FAR = \frac{False\ Alarms}{Hits + False\ Alarms} \quad (4)$$

$$BIAS = \frac{Hits + False\ Alarms}{Hits+Misses} \quad (5)$$

$$CSI = \frac{Hits}{Hits + False\ Alarms + Misses} \quad (6)$$

3. Results

3.1. Mamminasata Rainfall Pattern

Rainfall data from observations and CHIRPS rainfall estimates are calculated every 10 days, commonly called a decade, and monthly rainfall is used as the basis for grouping rainfall patterns. In areas near the coast with low topography, it is generally included in group 3, except for the northern part. The rainfall pattern is included in the second group in the northern part of Maros Regency. This group 2 rainfall pattern generally occurs in areas with elevations between 5 and 500 meters. The first pattern is in the northernmost region of Maros and one location in southern Gowa, as shown in Figure 2(a).

Edelweiss Applied Science and Technology
ISSN: 2576-8484
Vol. 8, No. 6: 9555-9567, 2024
DOI: 10.55214/25768484.v8i6.4035

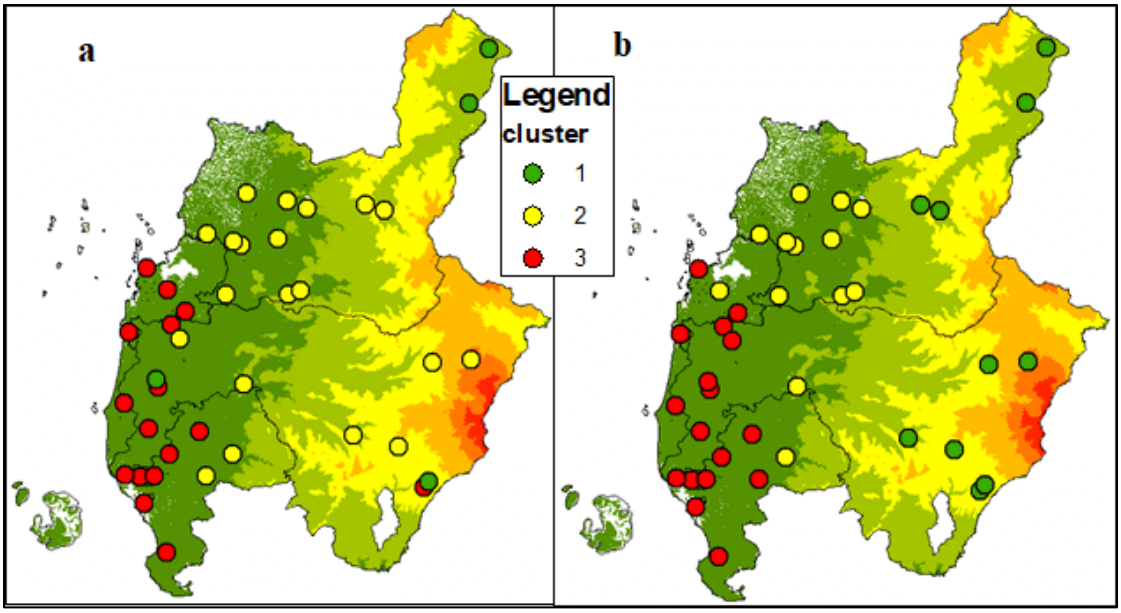

Figure 2.
Rainfall pattern in Mamminasata based on observation (a), and CHIRPS (b)

In contrast to the observed rainfall pattern, the CHIRPS rainfall pattern is more evident in its rainfall cluster group. Although the patterns are generally similar, the differences between the three patterns are more precise. The third pattern is in coastal lowlands that are less than 50 meters, while the first pattern is in mountainous areas with elevations of more than 200 meters. The second cluster is between the first and third clusters, situated between 50 and 200 meters, as shown in Figure 2(b). No anomalies were found in CHIRPS rainfall, where mountainous areas with rainfall patterns were included in group 2 or lowland areas with rainfall patterns in group 3. Nineteen locations were not the same as observed, and CHIRPS rainfall patterns.

3.2. Rainfall Pattern of CHIRPS vs Observation

Based on the rainfall graph every 10 days or decade, the rainfall graphic pattern in the Mamminasata rainfall decreases in the middle of the year and increases at the end and beginning of the year. The first pattern includes the areas of Tinggimoncong/BBI Kentang, BPP Mallawa, Gatareng Matinggi, and BPP Bulluballea, with rainfall at the beginning or end of the year ranging from 80-110 mm each and decreasing after March or the 9th date but increasing again in May through mid-June and then decreasing in the dry season. The second pattern includes the areas of Paranglompoa/Paladingan, for example, SMPK BB Malino/BPP Tinggi Moncong, BB Garing, etc. SMPK BPP Malakaji, BPP Cenrana, and Kappang have slightly lower rainfall intensity than the first pattern. Meanwhile, the third pattern has rainfall exceeding 100 mm each month at the beginning or end of the year and decreasing after February, reaching its lowest point in August or the 23rd month. At the end of the year, the rainfall pattern remains the same, increasing exponentially, as seen in Figure 3.

Edelweiss Applied Science and Technology
ISSN: 2576-8484
Vol. 8, No. 6: 9555-9567, 2024
DOI: 10.55214/25768484.v8i6.4035

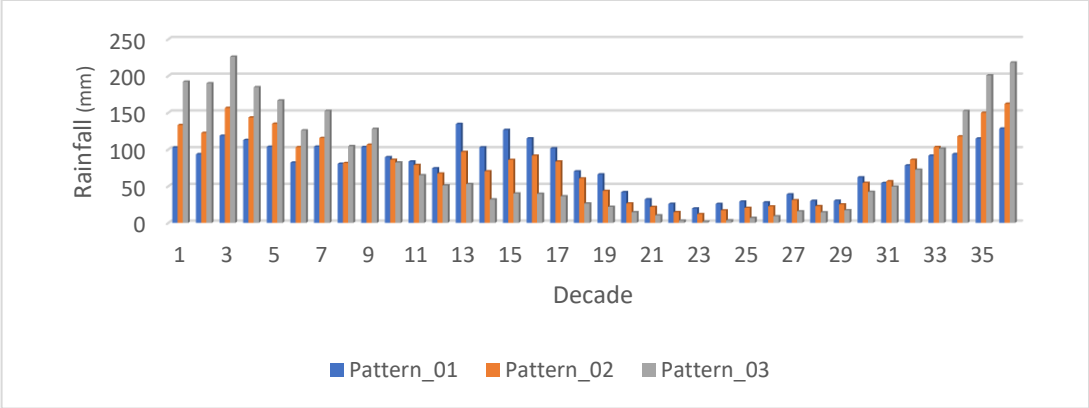

Figure 3.
Decade CHIRPS rainfall distribution.

Compared to the surface rainfall observation, CHIRPS underestimated rainfall at the beginning of the year, then overestimated during the dry season and approached the observed value at the end of the year, as shown in Figure 4. In general, the first pattern to the third pattern of observed rainfall is almost the same as CHIRPS, where there is an increase in rainfall intensity at the time of the transition from the rainy season to dry or on the 14th or 15th base. Entering the dry season, rainfall intensity should decrease, but at the first and second patterns rise about 50 mm on the 14th or 15th bottom.

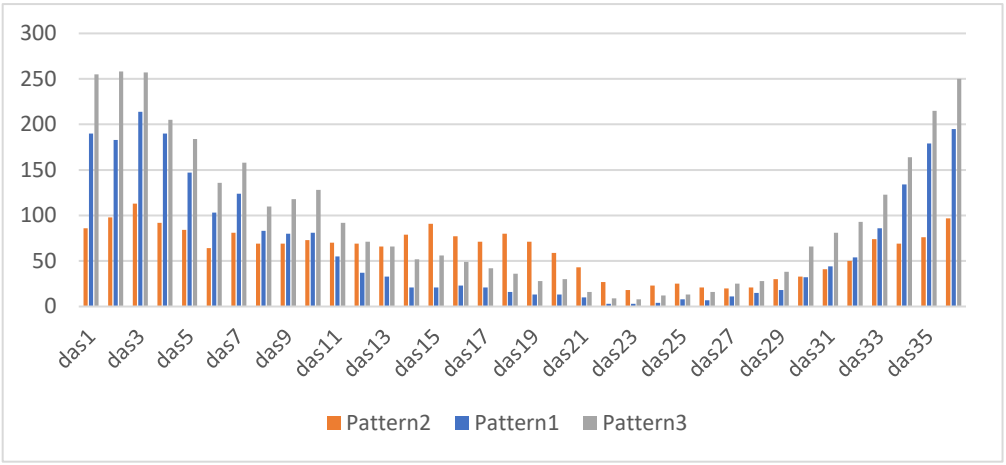

Figure 4.
Decade of rainfall surface observation.

The comparison of annual rainfall accumulation is the same for the entire Mamminasata Region, almost the same as in Figure 5. The lowest rainfall occurred in 1982 and 1997, with a value of less than 2000 mm/year, and was an extreme El Nino year. Meanwhile, annual rainfall reaching more than 3000 mm/year occurred in 1984, 1995, 1999, 2001, 2010, and 2017 during weak to substantial La-Nina periods.

Edelweiss Applied Science and Technology
ISSN: 2576-8484
Vol. 8, No. 6: 9555-9567, 2024
DOI: 10.55214/25768484.v8i6.4035

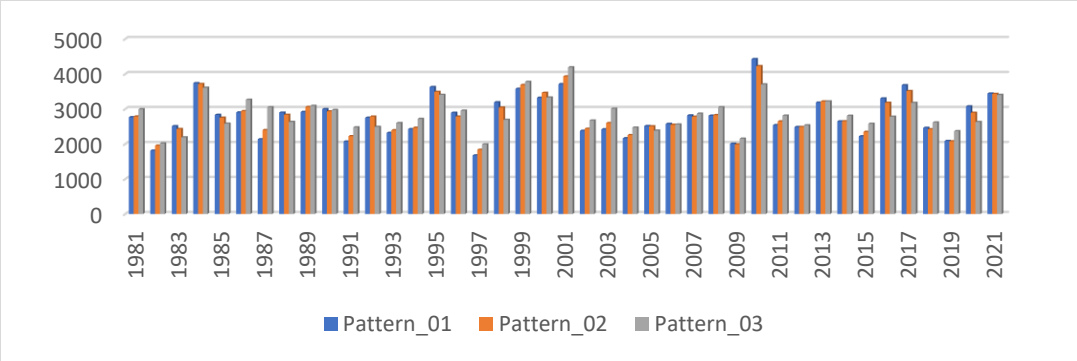

Figure 5.
Yearly distribution of CHIRPS rainfall estimates.

Based on the annual rainfall distribution, data for Tinggimoncong/BBI Kentang, BPP Mallawa, Gatareng Matinggi, and Bpp. Bulluballea, representing the first pattern, was not installed from 1981 to 1990, and data was cut off from 1997 to 2004. The CHIRPS annual rainfall estimate is generally overestimated, where the estimated annual rainfall is usually more than 2500 mm/year, while the results of observations on rains in the first and second pattern values less than 2000 mm/year, especially between 2006 and 2006. The first and second rainfall patterns are in the hills covering Paranglompoa/Paladingan. SMPK BB Malino/BPP Tinggi Moncong, Tinggimoncong/BBI Potato, BB Garing, ex. BPP SMPK Malakaji, BPP Cenrana, Kappang, BPP Mallawa, Gatareng Matinggi, and Bpp. Bullubalea is shown in Figure 6.

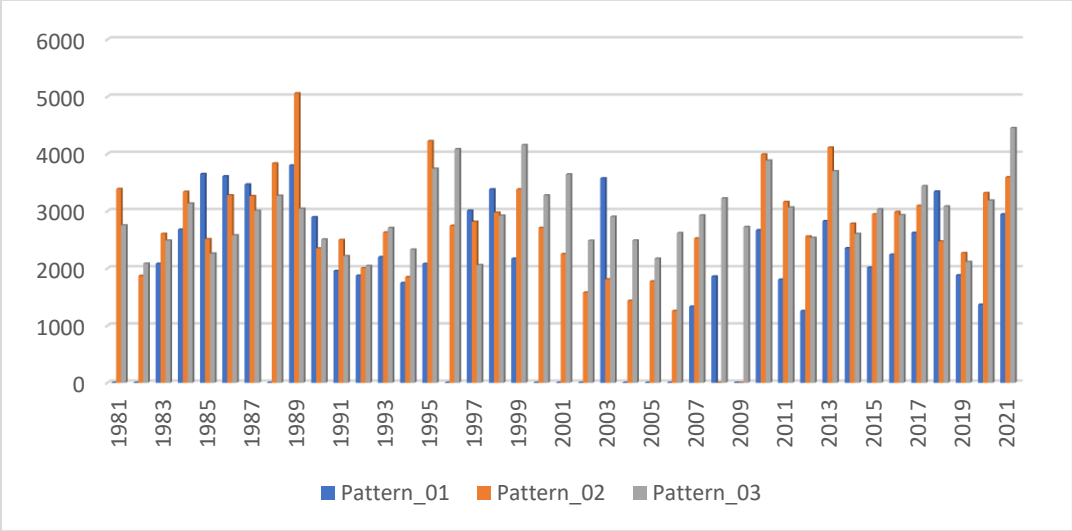

Figure 6.
Yearly distribution of rainfall surface observation.

3.3. Accuracy of CHIRPS

Based on the indicators of the dichotomous method, the percent correct, or PC value of CHIRPS is between 0.50 and 0.73. Accuracy or PC in areas close to the coast with elevations between 5 and 50 meters is generally higher than those with higher elevations. Figure 7 on the left shows a decreasing gradation of the percent correct (PC) concerning elevation. Mountainous areas over 1000 meters in height have the smallest percent correct values. However, it was found that there were locations that were very close but had different percent correct values. The condition of the various PC values is probably due to an incident where the first location recorded rain while other locations had no rain, or

Edelweiss Applied Science and Technology
ISSN: 2576-8484
Vol. 8, No. 6: 9555-9567, 2024
DOI: 10.55214/25768484.v8i6.4035

the rain event was random.

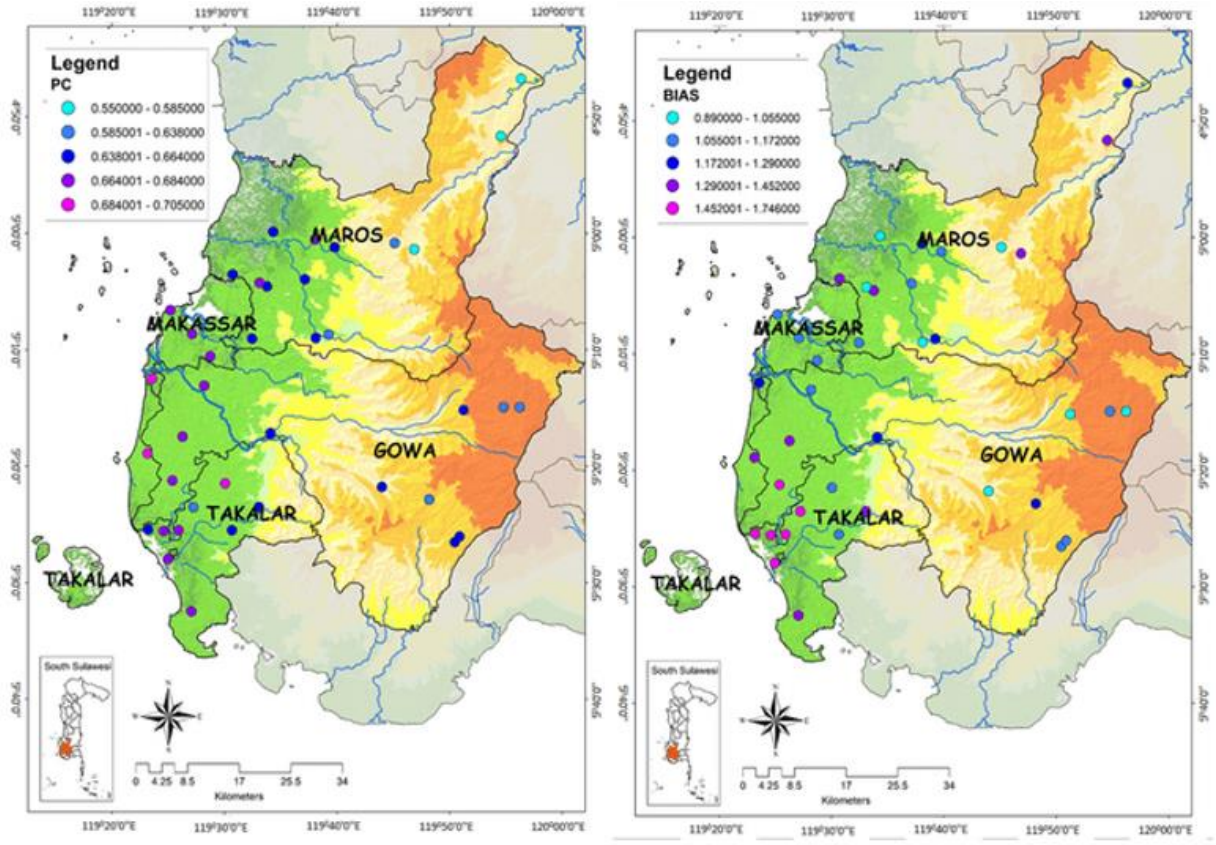

Figure 7.
Perform CHIRPS based on (a) Percent Correct (PC) and (b) Bias (BIAS)mn

The number of false alarms on the southwestern coast of Mamminasata was more significant than the missing ones, which means that CHIRPS estimates that many errors were made in warnings. The number of events predicted by CHIRPS would be rain, but the observations at that location did not occur more rain than the prediction error would not happen rain, but the observations did rain. Meanwhile, the opposite occurs in the northern part of the city and mountainous areas east of the town, where the number of missing items is higher than the number of false alarms. The same as the PC value, several locations had different bias values even though their locations were close. Even though the number of false alarm errors is more significant, they do not occur in every area. The comparison between false or missing alarms and the number of hits can be seen in the value of FAR and POD in Figure 8.

Edelweiss Applied Science and Technology
ISSN: 2576-8484
Vol. 8, No. 6: 9555-9567, 2024
DOI: 10.55214/25768484.v8i6.4035

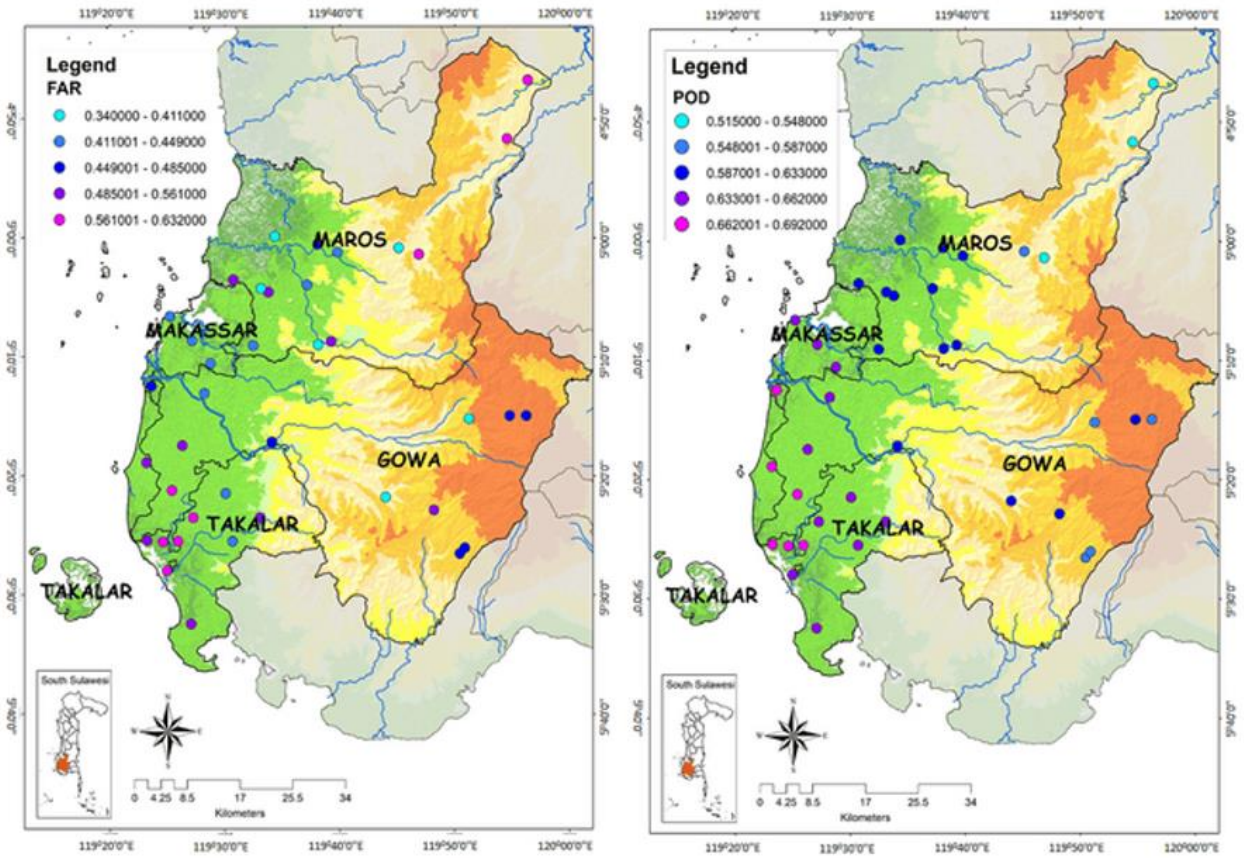

Figure 8.
Perform CHIRPS based on (a) FAR and (b) POD

CHIRPS rainfall prediction errors are always present at all locations based on the number of missing or false alarms. Based on Figure 8, the proportion of the number of false alarms is in the area around Takalar or southwest of Mamminasata and the mountainous regions with higher elevations than 1000 m, while the least number of false alarms is in the north of the city where the FAR value is less than 0.5. The proportion of errors due to missing hits identified from the POD value shows that in the area around Takalar or southwest of Mamminasata, it is small compared to the northern part of the city and mountains with a POD value of more than 0.5.

Based on the proportion of the number of hits to all predictions, the northern area of Mamminasata is better with a higher CSI value than other areas, as shown in Figure 9. The relatively mountainous area has a CSI value of more than 0.36. In contrast, the proportion of hits is more varied for the coastal area, with a tendency towards the southern area of Mamminasata being smaller than the northern area in Figure 9.

Edelweiss Applied Science and Technology
ISSN: 2576-8484
Vol. 8, No. 6: 9555-9567, 2024
DOI: 10.55214/25768484.v8i6.4035

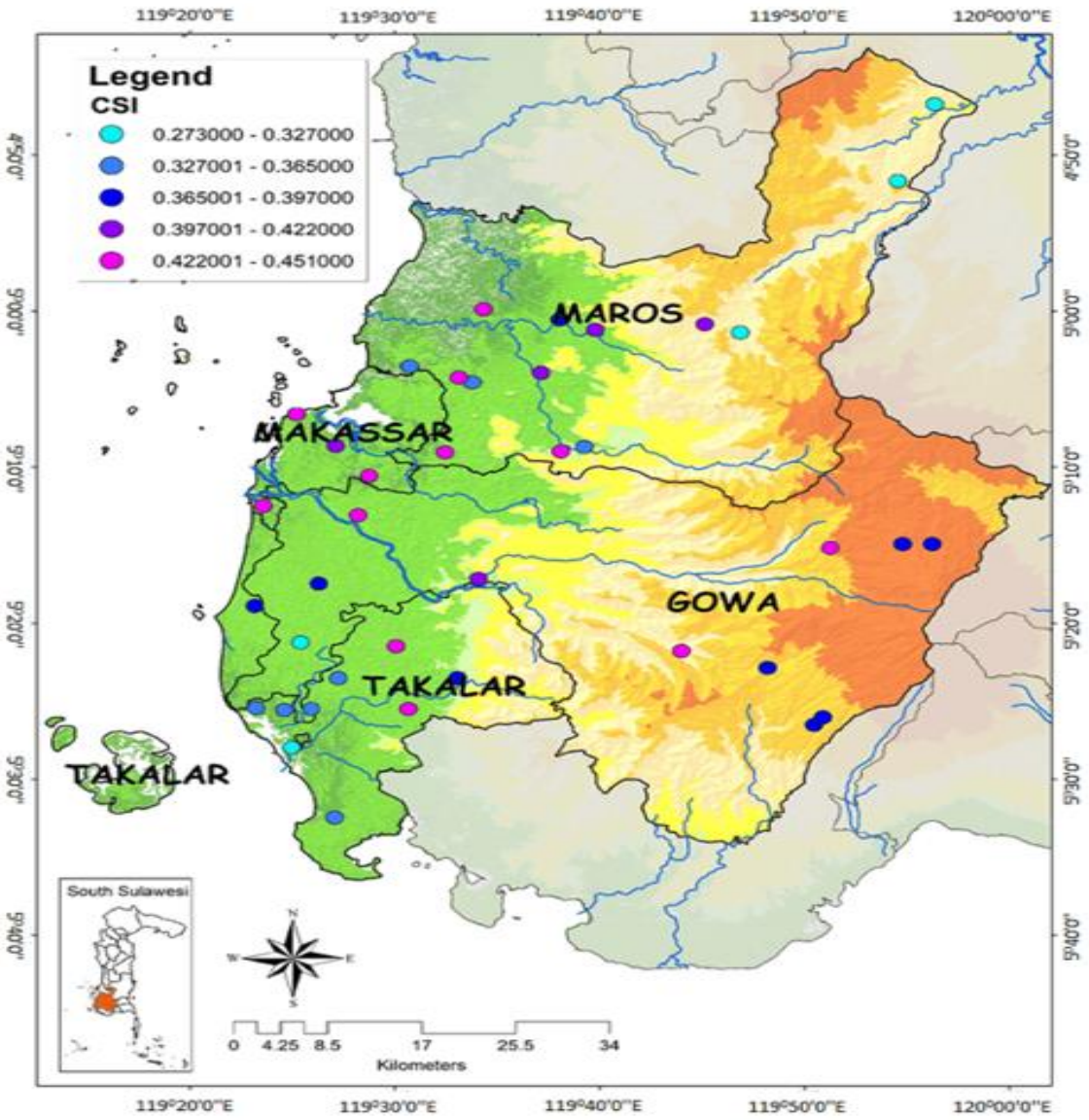

Figure 9.
Perform CHIRPS based on CSI.

4. Discussion

There is no robust network of meteorological stations in Indonesia, including the Mamminasata region, and no homogenous distribution throughout the territory. Therefore, other observation sources, such as satellite data, can be considered. Products with long records, such as the Climate Hazards Group Infrared Precipitation with Stations (CHIRPS), can be used to help with weather or climate analysis [37], [38]. Comparing CHIRPS daily precipitation estimates with rain gauges in China showed better in areas with high precipitation than in arid and semi-arid lands [28]. These rainfall estimates perform well in monthly rainfall, although slightly overestimating total precipitation [29], [39]. The CHIRPS data can capture spatial rainfall distribution in watershed areas [20], [40]. However, this product tends to be underestimated compared to the ground-based measurements in all seasons and will perform in the land regions and worse at higher elevations. This research confirms that high elevation overestimates CHIRPS rainfall.

Edelweiss Applied Science and Technology
ISSN: 2576-8484
Vol. 8, No. 6: 9555-9567, 2024
DOI: 10.55214/25768484.v8i6.4035

Compared to other satellite rainfall estimates, CHIRPS best estimates rainfall in the arid, hot tropical climate and could, therefore, be used for studies related to drought and irrigation [41], [42]. However, CHIRPS can tend to underestimate in the rainiest months, especially during high rainfall (>100mm/month) and its ability to detect rain is poor in areas above 1000 mean sea level [43]. Based on research by Baez-Villanueva et al. (2018), the performance of rainfall CHIRPS estimates is affected by climatic and geographic characteristics. These rainfall estimates also produced a more realistic representation of rainfall despite the recurring spatial limitations in regions with contrasting emissivity, temperature, and orography [44]. Some research found that CHIRPS was one of the products that underestimated extreme precipitation values and had a lower correlation coefficient for maximum values [45]- [46].

Evaluation of daily rainfall CHIRPS estimates in Mamminasata, part of the Indonesian tropical maritime continent has a percent correct (PC) value of 0.5 to 0.73. PC accuracy in areas close to the coast at low elevations is generally higher than those with higher elevations. CHIRPS' predictions tended to be overestimated on the southwestern coast of Mamminasata. In contrast, the northern part of the city and mountainous areas east of the town tended to be underestimated. Based on the proportion of the number of hits to all predictions, the CSI value is higher in the northern area of Mamminasata than in other areas. Several lower-than-the-calculated indicators must be considered to anticipate flooding, especially in densely populated areas [13]. Based on the calculation accuracy, CHIRPS's estimated rainfall is quite suitable for areas around the coast, but the accuracy is lower in areas with higher elevations.

5. Conclusions

Based on a comparison of rainfall CHIRPS estimates and surface rainfall data observation for 30 years in the monsoonal area Mamminasata, it can be concluded that:

1. Rainfall data from observations and CHIRPS have a similar pattern. There is a rainfall pattern in areas near the coast with low topography, areas with elevations between 50 and 200 meters, and mountainous areas.
2. CHIRPS rainfall estimates in the Mamminasata region have three rainfall patterns identified through observational data and further explained with CHIRPS data. The first is a typical monsoonal rainfall pattern, where rainfall is high at the beginning of the year, decreases in the middle of the year, and increases at the end. The second pattern is high rainfall at the beginning or end of the year, each between 80-110 mm, and decreases after March. Furthermore, there is an increase from May to mid-June, which then decreases afterward. The third pattern has the same pattern as the second pattern, but its intensity is 30% lower.
3. The accuracy of rainfall estimates using satellites varies significantly in the Mamminasata area. Generally, the performance of CHIRPS rainfall estimates is better in lowland areas than in mountainous areas. The percent correct (PC) is between 0.50 and 0.73 and performs better along the lowland coastal areas. However, CHIRPS predictions lean towards overestimation in the southwestern coastal zone, and the northern urban and eastern mountainous regions tend to underestimate.

Acknowledgments:
We want to thank Hasanuddin University's leadership, which has provided these research facilities. This research activity is supported through Professors Grant of Hasanuddin University No: 03092/UN4.1/KEP/2024.

References

[1] R. D'Arrigo and R. Wilson, El Nino and Indian Ocean influences on Indonesian drought: implications for forecasting rainfall and crop productivity, Int. J. Climatol. A J. R. Meteorol. Soc., vol. 28, no. 5, pp. 611–616, 2008. DOI: 10.1002/joc.1654

[2] R. Hidayat and S. Kizu, Influence of the Madden–Julian Oscillation on Indonesian rainfall variability in austral summer, Int. J. Climatol., vol. 30, no. 12, pp. 1816–1825, 2010. DOI: 10.1002/joc.2005

[3] R. Hidayat, M. D. Juniarti and U. Ma'rufah, Impact of La Niña and La Niña Modoki on Indonesia rainfall variability, IOP Conf. Ser.: Earth Environ. Sci. 149 012046, 2018. **DOI** 10.1088/1755-1315/149/1/012046

[4] H. S. Lee, General rainfall patterns in Indonesia and the potential impacts of local season rainfall intensity, Water, vol. 7, no. 4, pp. 1751–1768, 2015. https://doi.org/10.3390/w7041751

[5] M. Martono and T. Wardoyo, Impacts of El Niño 2015 and the Indian Ocean Dipole 2016 on rainfall in the Pameungpeuk and Cilacap regions, in Forum Geografi, 2017, pp. 184–195.

[6] Y. Yang and Y. Song, Application of Poisson Process to Drought Prediction – the Case Study of Yucheng City, Int. Arch. Photogramm. Remote Sens. Spat. Inf. Sci., vol. XLVIII-3/W, no. November, pp. 73–78, 2022, doi: 10.5194/isprs-archives-xlviii-3-w1-2022-73-2022.

[7] L. R. Iksanti and D. Maulana, Lion Air's Strategy in Increasing Domestic Aviation Market Share at Makassar's Sultan Hasanuddin International Airport. JETISH: Journal of Education Technology Information Social Sciences and Health, vol 2, no. 2, pp. 1421-1428, 2023.

[8] A. Anirwan, Urbanization and Climate Resilience: How is Vulnerability and Poverty in Makassar. J. Gov., vol. 8, no. 2, 2023.

[9] M. Siki, A. A., Samudra, Andriansyah and A. Suradika, Management of the Distribution of Logistics Assistance for Disaster Survivors: Study on the Makassar Flood in South Sulawesi. The Social Perspective Journal, vol. 2, No.2, pp. 131–145, 2023.

[10] I. Ismayanti and A. M. A. Aljurida, Urgency in Urban Flood Disaster Mitigation: Response and Policy Initiation by Makassar City Government. Journal of Governance and Local Politics (JGLP), vol. 5, No. 2, 155-163, 2023.

[11] M. I. Thoban and D. R. Hizbaron, Urban resilience to floods in parts of Makassar, Indonesia. E3S Web Conf. The 1st Geosciences and Environmental Sciences Symposium (ICST 2020), vol. 200, 2020.

[12] Giarno, M. Muflihah, and M. Mujahidin, Determination of Optimal Rain Gauge on The Coastal Region Use Coefficient Variation: Case Study in Makassar, in Journal of the Civil Engineering Forum, 2021, pp. 121–132.

[13] N. Sunusi, "Comparison of some schemes for determining the optimal number of rain gauges in a specific area: A case study in an urban area of South Sulawesi, Indonesia, AIMS Environ. Sci., vol. 9, no. 3, 2022. DOI. 10.3934/environsci.2022018.

[14] C. Kidd, D. R. Kniveton, M. C. Todd, and T. J. Bellerby, Satellite rainfall estimation using combined passive microwave and infrared algorithms, J. Hydrometeorol., vol. 4, no. 6, pp. 1088–1104, 2003. DOI: https://doi.org/10.1175/1525-7541(2003)004<1088:SREUCP>2.0.CO;2

[15] D. B. Wright, R. Mantilla, and C. D. Peters-Lidard, A remote sensing-based tool for assessing rainfall-driven hazards," Environ. Model. Softw., vol. 90, pp. 34–54, 2017. https://doi.org/10.1016/j.envsoft.2016.12.006

[16] Giarno, M. P. Hadi, S. Suprayogi, and S. Herumurti, Impact of rainfall intensity, monsoon and MJO to rainfall merging in the Indonesian maritime continent, J. Earth Syst. Sci., vol. 129, no. 1, p. 164, 2020. https://doi.org/10.1007/s12040-020-01427-8

[17] Giarno, M. P. Hadi, S. Suprayogi, and S. Herumurti, Bias correction of radar and satellite rainfall estimates and increasing its accuracy using modified merging, Mausam, vol. 71, no. 3, pp. 377–390, 2020. DOI: https://doi.org/10.54302/mausam.v71i3.36

[18] D. W. Martin and W. D. Scherer, Review of satellite rainfall estimation methods," Bull. Am. Meteorol. Soc., vol. 54, no. 7, pp. 661–675, 1973. DOI: https://doi.org/10.1175/1520-0477-54.7.661

[19] N. K. Shrestha, F. M. Qamer, D. Pedreros, M. S. R. Murthy, S. M. Wahid, and M. Shrestha, "Evaluating the accuracy of Climate Hazard Group (CHG) satellite rainfall estimates for precipitation based drought monitoring in Koshi basin, Nepal," J. Hydrol. Reg. Stud., vol. 13, pp. 138–151, 2017. https://doi.org/10.1016/j.ejrh.2017.08.004

[20] M. N. Islam and H. Uyeda, Use of TRMM in determining the climatic characteristics of rainfall over Bangladesh, Remote Sens. Environ., vol. 108, no. 3, pp. 264–276, 2007. https://doi.org/10.1016/j.rse.2006.11.011

[21] M. O. Karaseva, S. Prakash, and R. M. Gairola, Validation of high-resolution TRMM-3B43 precipitation product using rain gauge measurements over Kyrgyzstan, Theor. Appl. Climatol., vol. 108, pp. 147–157, 2012. https://doi.org/10.1007/s00704-011-0509-6

[22] S. Sorooshian et al., Diurnal variability of tropical rainfall retrieved from combined GOES and TRMM satellite information, J. Clim., vol. 15, no. 9, pp. 983–1001, 2002.

[23] S. Moazami, S. Golian, M. R. Kavianpour, and Y. Hong, Comparison of PERSIANN and V7 TRMM Multi-satellite Precipitation Analysis (TMPA) products with rain gauge data over Iran," Int. J. Remote Sens., vol. 34, no. 22, pp. 8156–8171, 2013. https://doi.org/10.1080/01431161.2013.833360

[24] A. K. Shukla, C. S. P. Ojha, and R. D. Garg, Geo-spatial Approach for Estimation of Precipitation over the Upper Ganga River Basin (UGRB), Uttarakhand, India, Indian J. Sci. Technol., vol. 9, p. 48, 2016.

[25] R. J. Joyce, J. E. Janowiak, P. A. Arkin, and P. Xie, CMORPH: A method that produces global precipitation estimates from passive microwave and infrared data at high spatial and temporal resolution, J. Hydrometeorol., vol. 5, no. 3, pp. 487–503, 2004. DOI: https://doi.org/10.1175/1525-7541(2004)005<0487:CAMTPG>2.0.CO;2

[26] L. Bai, C. Shi, L. Li, Y. Yang, and J. Wu, Accuracy of CHIRPS satellite-rainfall products over mainland China," Remote Sens., vol. 10, no. 3, p. 362, 2018.https://doi.org/10.3390/rs10030362.
[27] F. Gao et al., Comparison of two long-term and high-resolution satellite precipitation datasets in Xinjiang, China, Atmos. Res., vol. 212, pp. 150–157, 2018. https://doi.org/10.1016/j.atmosres.2018.05.016
[28] Giarno. Clustering Pandemic COVID-19 and Relationship to Temperature and Relative Humidity Among the Tropic and Subtropic Region; Walailak Journal of Science and Technology (WJST) 18(17) Article 9750 (13 pages), https://doi.org/10.48048/wjst.2021.9750
[29] Gokila, S., Kumar, K. A. and Bharath, A. 2015 Clustering and classification in support of climatology to mine weather data: A review; Int. J. Comput. Algorithm. 4 45-8. https://doi.org/10.20894/IJCOA.101.004.001.011.
[30] Komalasari, K. E., Pawitan, H. and Faqih, A. 2017, Descriptive Statistics and Cluster Analysis for Extreme Rainfall in Java Island; IOP Conf. Ser.: Earth Environ. Sci. 58 012039 https://doi.org/10.1088/1755-1315/58/1/012039.
[31] Kuswanto, H., Setiawan, D. and Sopaheluwakan, A. 2019 Clustering of Precipitation Pattern in Indonesia Using TRMM Satellite Data; Eng. Technol. Appl. Sci. Res. 9(4) 4484–4489. https://doi.org/10.48084/etasr.2950
[32] Marzban, C. and Sandgathe, S. 2006 Cluster analysis for verification of precipitation fields; Weather Forecast, 21, 824–38. https://doi.org/10.1175/WAF948.1
[33] Murugesakumar, B., Anandakumar, K. and Bharathi, A. 2017 Improved fuzzy K-means cluster algorithm to analyse weather data in coimbatoreregion; Int. J. Adv. Eng. Res. Dev., 4, 840-6. https://doi.org/10.1109/CCIS.2018.8691136.
[34] Bayong Tjasyono HK., 2004. Climatology, ITB Publishing, Bandung.
[35] Didiharyono and Giarno. Application of the simple verification method to estimate the weather at makassar maritime station, Indonesia," Walailak J. Sci. Technol., vol. 18, no. 18, pp. 9512–9542, 2021. **DOI:** https://doi.org/10.48048/wjst.2021.9542
[36] C. Funk et al. The climate hazards infrared precipitation with stations—a new environmental record for monitoring extremes. Sci. data, vol. 2, no. 1, pp. 1–21, 2015.
[37] C. Funk, A. Verdin, J. Michaelsen, P. Peterson, D. Pedreros, and G. Husak, A global satellite-assisted precipitation climatology, Earth Syst. Sci. Data, vol. 7, no. 2, pp. 275–287, 2015.
[38] W. Wu, Y. Li, X. Luo, Y. Zhang, X. Ji, and X. Li. Performance evaluation of the CHIRPS precipitation dataset and its utility in drought monitoring over Yunnan Province, China. Geomatics, Nat. Hazards Risk, vol. 10, no. 1, pp. 2145–2162, 2019. https://doi.org/10.1080/19475705.2019.1683082
[39] J. A. Rivera, S. Hinrichs, and G. Marianetti. Using CHIRPS Dataset to Assess Wet and Dry Conditions along the Semiarid Central-Western Argentina. Adv. Meteorol., vol. 2019, no. 1, p. 8413964, 2019. https://doi.org/10.1155/2019/8413964
[40] F. Zambrano, B. Wardlow, T. Tadesse, M. Lillo-Saavedra, and O. Lagos. Evaluating satellite-derived long-term historical precipitation datasets for drought monitoring in Chile. Atmos. Res., vol. 186, pp. 26–42, 2017. https://doi.org/10.1016/j.atmosres.2016.11.006
[41] R. B. Lopes Cavalcante, D. B. da Silva Ferreira, P. R. Monteiro Pontes, R. G. Tedeschi, C. P. Wanzeler da Costa, and E. B. de Souza. Evaluation of extreme rainfall indices from CHIRPS precipitation estimates over the Brazilian Amazonia. Atmos. Res., vol. 238, 2020. https://doi.org/10.1016/j.atmosres.2020.104879
[42] J. M. Macharia, F. K. Ngetich, and C. A. Shisanya. Comparison of satellite remote sensing derived precipitation estimates and observed data in Kenya. Agric. For. Meteorol., vol. 284, p. 107875, 2020. https://doi.org/10.1016/j.agrformet.2019.107875
[43] F. J. Paredes-Trejo, H. A. Barbosa, and T. V. L. Kumar. Validating CHIRPS-based satellite precipitation estimates in Northeast Brazil. J. Arid Environ., vol. 139, pp. 26–40, 2017. https://doi.org/10.1016/j.jaridenv.2016.12.009
[44] F. Satgé, D. Ruelland, M.-P. Bonnet, J. Molina, and R. Pillco. Consistency of satellite-based precipitation products in space and over time compared with gauge observations and snow-hydrological modelling in the Lake Titicaca region. Hydrol. Earth Syst. Sci., vol. 23, no. 1, pp. 595–619, 2019. https://doi.org/10.5194/hess-23-595-2019
[45] R. S. A. Palharini et al., "Assessment of the extreme precipitation by satellite estimates over South America," Remote Sens., vol. 12, no. 13, p. 2085, 2020. https://doi.org/10.3390/rs12132085